Rapid Communications

Resistivity anisotropy of quantum Hall stripe phases

M. Sammon,[1,*] X. Fu,[1] Yi Huang (黄奕),[1] M. A. Zudov,[1] B. I. Shklovskii,[1] G. C. Gardner,[2,3] J. D. Watson,[3,4,†] M. J. Manfra,[2,3,4,5] K. W. Baldwin,[6] L. N. Pfeiffer,[6] and K. W. West[6]

[1]*School of Physics and Astronomy, University of Minnesota, Minneapolis, Minnesota 55455, USA*
[2]*Microsoft Quantum Lab Purdue, Purdue University, West Lafayette, Indiana 47907, USA*
[3]*Birck Nanotechnology Center, Purdue University, West Lafayette, Indiana 47907, USA*
[4]*Department of Physics and Astronomy, Purdue University, West Lafayette, Indiana 47907, USA*
[5]*School of Electrical and Computer Engineering and School of Materials Engineering, Purdue University, West Lafayette, Indiana 47907, USA*
[6]*Department of Electrical Engineering, Princeton University, Princeton, New Jersey 08544, USA*

(Received 3 October 2019; published 20 December 2019)

Quantum Hall stripe phases near half-integer filling factors $\nu \geqslant 9/2$ were predicted by Hartree-Fock (HF) theory and confirmed by discoveries of giant resistance anisotropies in high-mobility two-dimensional electron gases. A theory of such anisotropy was proposed by MacDonald and Fisher, although they used parameters whose dependencies on the filling factor, electron density, and mobility remained unspecified. Here, we fill this void by calculating the hard-to-easy resistivity ratio as a function of these three variables. Quantitative comparison with experiment yields very good agreement, which we view as evidence for the "plain vanilla" smectic stripe HF phases.

DOI: 10.1103/PhysRevB.100.241303

Quantum Hall stripe phases near half-integer filling factors $\nu \geqslant 9/2$ were predicted for spin-split Landau levels (LLs) by the Hartree-Fock (HF) theory [1–3]. At exactly half-integer filling factor ν, these phases consist of alternating stripes with filling factors $\nu - 1/2$ and $\nu + 1/2$, both with the width $\Lambda/2 \simeq 1.4R_c$ [1,2,4,5], where R_c is the cyclotron radius (see Fig. 1). These stripes are formed due to the repulsive boxlike screened interaction potential of electrons with ringlike wave functions in high LLs. Such a potential leads to an energy gain when electrons occupy the nearest states of the same stripe and avoid interacting with electrons in neighboring stripes. The self-consistent HF theory is valid at LL indices $N \gg 1$, when $R_c = l_B(2N+1)^{1/2} \gg l_B$. Here, $l_B = (c\hbar/eB)^{1/2}$ is the magnetic length, which is a measure of quantum fluctuations of an electron's cyclotron orbit center. It was shown [2,4,5] that quantum fluctuations play little role even when $N = 2$, so that stripes should determine ground states for all half-integer $\nu \geqslant 9/2$.

Quantum Hall stripes were confirmed by discoveries of dramatic resistance anisotropies in high-mobility two-dimensional electron gases (2DEGs) hosted in GaAs/AlGaAs heterostructures at $\nu = 9/2, 11/2, 13/2, \ldots$ [6,7]. The preferred direction of the stripes (symmetry breaking) was found to be imposed by a potential related to GaAs crystal orientation, whose origin is not understood even now.

MacDonald and Fisher (MF) proposed a theory of the stripe phase conductivity [8]. They assumed that stripes form a smectic state, pinned by disorder, and used an analogy between stripe edges and edge states in a confined 2DEG (see Fig. 1). At half-integer filling factors $\nu \geqslant 9/2$ this theory leads to the resistivity ratio

$$\frac{\rho_{xx}}{\rho_{yy}} = \left(\frac{v\tau_B}{\Lambda}\right)^2 \gg 1, \tag{1}$$

where $\Lambda \simeq 2.8R_c$ is the stripe period, v is the drift velocity of electrons on the stripe edges (see Fig. 1), and τ_B is the time of an electron scattering to a neighboring stripe edge. Let us interpret Eq. (1). An electron drifts for a time $\tau_B/2$ until it is scattered to one of the adjacent edges. Thus, we can define two electron diffusion constants,

$$D_{xx} = \frac{1}{2}\frac{(\Lambda/2)^2}{\tau_B/2} = \frac{\Lambda^2}{4\tau_B}, \tag{2}$$

$$D_{yy} = \frac{1}{2}\frac{(v\tau_B/2)^2}{\tau_B/2} = \frac{v^2\tau_B}{4}. \tag{3}$$

Here, we have used the fact that at each time step $\tau_B/2$ an electron on the edge of a stripe randomly moves a distance $v\tau_B/2$ in the y direction, while it hops a distance $\Lambda/2$ in the x direction. Taking the ratio of D_{yy} and D_{xx} and using the Einstein relationship we arrive at Eq. (1).

In its present form, Eq. (1) does not allow comparison with the experimental data, which we talk about below, as Ref. [8] did not specify how τ_B or v depend on the electron density n_e, the mobility μ, and the filling factor ν. In this Rapid Communication we calculate τ_B and v, and arrive at the ratio of resistivities which can be directly compared with experimental data,

$$\frac{\rho_{xx}}{\rho_{yy}} = \frac{0.088}{\gamma^2}\left(\frac{\hbar n_e \mu}{\pi^3 e\nu(2N+1)}\right)^2. \tag{4}$$

*Corresponding author: sammo017@umn.edu
†Present address: Microsoft Station-Q at Delft University of Technology, 2600 GA Delft, The Netherlands.

 ©2019 American Physical Society

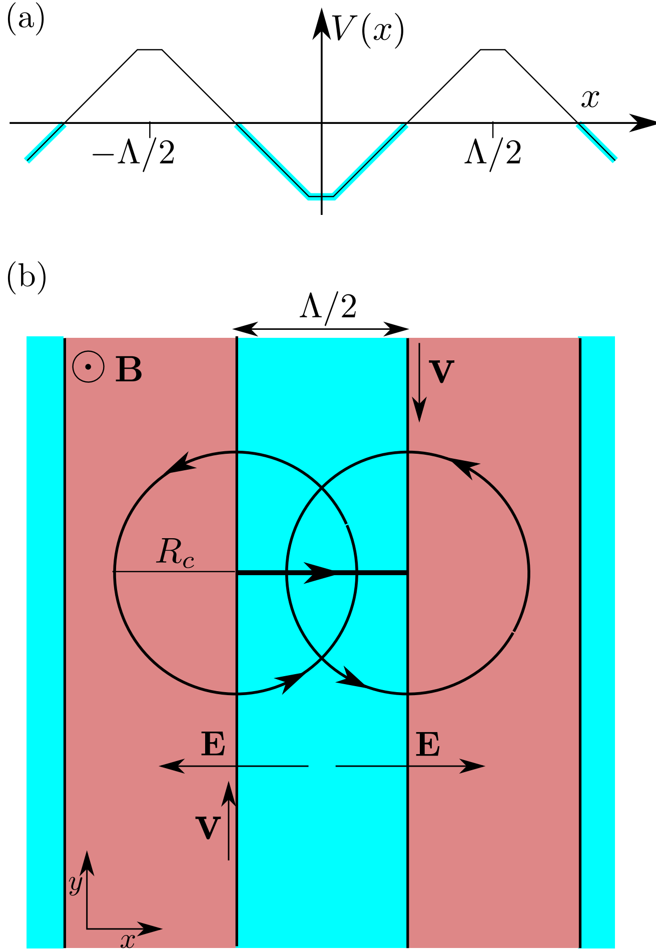

FIG. 1. (a) Schematic drawing of the single-particle self-consistent potential energy $V(x)$ which is responsible for stripe formation due to an approximate boxlike electron-electron interaction [2]. The sloped regions of $V(x)$ determine the internal electric field E. (b) Schematic of transport in the stripe phase. Electrons on the stripe edges (shown in blue) drift in electric fields E with velocity v in the $\pm y$ direction. They are scattered to an adjacent stripe edge by background charged impurities at a rate $2/\tau_B$, as illustrated by the thick horizontal arrow.

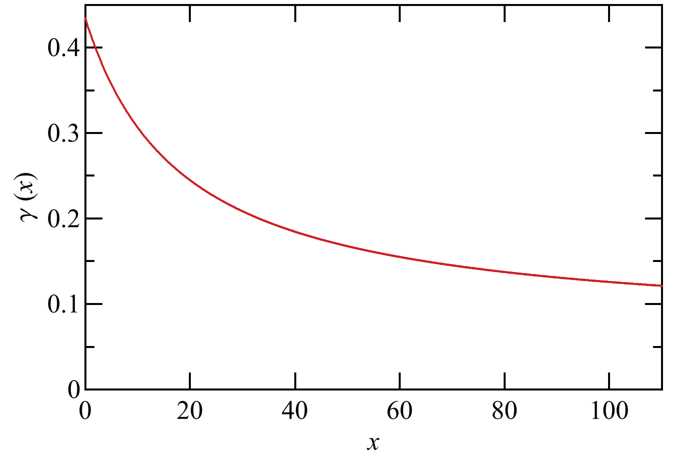

FIG. 2. $\gamma(x)$ for electron density $n_e = 3\times10^{11}$ cm^{-2} and quantum well width $w = 30$ nm.

Here, $\nu \geqslant 9/2$ is either $2N+1/2$ or $2N+3/2$ and $\gamma \equiv \gamma(N_1/N_2)$ is a dimensionless function of concentrations N_1 and N_2 of unintentional background impurities in the $Al_xGa_{1-x}As$ spacer and GaAs quantum well, correspondingly. We focus on ultrahigh mobility 2DEG in which the long-range potential of remote donors plays a minor role for the momentum relaxation time τ and τ_B. It is easy to see from Eq. (4) that $\rho_{xx}/\rho_{yy} \propto \mu^2 B^4/n_e^2$ at $N \gg 1$. We show below that this prediction for high LL agrees with experiment and arrive at $N_1/N_2 \simeq 60$ using N_1/N_2 as a single fitting parameter.

Let us now derive our expressions for v and τ_B which allow the conversion of Eq. (1) into Eq. (4). The drift velocity is $v = cE/B$, where B is the magnetic field, $eE = |dV/dx|$ at $x = \pm\Lambda/4$ is the internal electric field at the stripe edges, and $V(x)$ is the self-consistent HF potential. Following MF, we assume that at low temperatures electrons form a smectic pinned by impurities. If we use the model of a sawtooth stripe potential $V(x)$ [Fig. 1(a)], based on the simplified box model of electron repulsive potential given by Eq. (15) of Ref. [2], we find $eE = \hbar\omega_c/2\pi^2 R_c$, where ω_c is cyclotron frequency. Below we use a more accurate expression

$$eE = \beta(r_s)\frac{\hbar\omega_c}{2\pi^2 R_c}, \tag{5}$$

where $\beta(r_s)$ can be obtained from Eqs. (48) and (43) of Ref. [2], $r_s \equiv (\pi n_e a_B^2)^{-1/2}$, $a_B = \hbar^2\kappa/m^\star e^2$, $m^\star$ is the effective mass, and κ is the dielectric constant of GaAs. The 2DEGs we consider have $r_s \simeq 1$ and $\beta(1) = 0.77$. Using Eq. (5) we find the drift velocity in Eq. (1),

$$v = \frac{cE}{B} = \frac{\beta}{2\pi^2}\frac{v_F}{\sqrt{\nu(2N+1)}}, \tag{6}$$

where v_F is the Fermi velocity. Next, we show that

$$\frac{2}{\tau_B} = \frac{\gamma}{\tau}\frac{g_B}{g_0}, \tag{7}$$

where $g_0 = m^\star/2\pi\hbar^2$ is the density of states per spin at $B = 0$, and

$$g_B = \frac{2}{2\pi l_B^2 eE\Lambda} = \frac{2}{h v \Lambda} \tag{8}$$

is the modified density of states at the Fermi level of the spin-polarized half-filled LL [see Fig. 1(a)], defined as the ratio of $(2\pi l_B^2)^{-1}$ and the energy width of a LL $eE\Lambda/2$ [2]. Apparently, in strong magnetic fields relatively narrow LLs, with $g_B/g_0 \gg 1$, are formed. This increases the scattering rate $2/\tau_B$ in comparison with $1/\tau$ [9] in Eq. (7). The dimensionless function $\gamma(N_1/N_2)$ in Eq. (7), shown in Fig. 2, takes care of relative contributions of the background charged impurities in the spacer and in the quantum well to $2/\tau_B$ and $1/\tau$ [10]. Combining Eqs. (1), (6), (7), and (8) we arrive at Eq. (4).

In the rest of this Rapid Communication we compare Eq. (4) with the experimental data from several high-mobility samples. The 2DEG in each of our three samples (A, B, C) resides in a GaAs quantum well surrounded by $Al_{0.24}Ga_{0.76}As$ barriers. Electrons are supplied by Si doping in narrow GaAs wells, surrounded by thin AlAs layers, and placed at a setback

TABLE I. Sample ID, electron density n_e, mobility μ, quantum well width w, setback distance d.

Sample ID	n_e (10^{11} cm^{-2})	μ (10^6 cm^2/V s)	w (nm)	d (nm)
A	2.9	28	30	75
B	2.8	16	30	75
C	3.0	16	30	80

distance d on each side of the GaAs well hosting the 2DEG. Sample parameters, such as density n_e, mobility μ, quantum well width w, and setback distance d are listed in Table I. The samples were ≈4–5 mm squares with eight contacts positioned at the corners and at the midsides. Resistances R_{xx} and R_{yy} were measured using a four-terminal, low-frequency (a few Hz) lock-in technique at temperature $T \approx 50$ mK for sample A and at $T \approx 25$ mK for samples B and C. The representative data for sample A are presented in Fig. 3.

For square sample geometry, resistivities ρ_{xx} and ρ_{yy} can be obtained from resistances R_{yy} and R_{xx} using [11]

$$R_{ii} = \frac{4}{\pi}\sqrt{\rho_{jj}\rho_{ii}} \sum_{n=\mathrm{odd}^+} \left[n \sinh\left(\frac{\pi n}{2}\sqrt{\frac{\rho_{jj}}{\rho_{ii}}} \right) \right]^{-1}, \quad (9)$$

where $i, j = x, y$ $(i \neq j)$. This equation assumes that the current is passed between midside contacts and the voltage is measured between corner contacts. With known R_{xx} and R_{yy}, Eq. (9) allows one to obtain the resistivity ratio ρ_{xx}/ρ_{yy} using

$$\frac{R_{xx}}{R_{yy}} = \frac{\sum_{n=\mathrm{odd}^+} \left[n \sinh\left(\frac{\pi n}{2\sqrt{\rho_{xx}/\rho_{yy}}} \right) \right]^{-1}}{\sum_{n=\mathrm{odd}^+} \left[n \sinh\left(\frac{\pi n \sqrt{\rho_{xx}/\rho_{yy}}}{2} \right) \right]^{-1}}. \quad (10)$$

Unfortunately, when R_{yy} becomes comparable to the experimental noise, direct application of Eq. (10) becomes unreliable. In such situations we resort to using the parameter-free result for the resistivity product $\rho_{xx}\rho_{yy}$ which was first obtained by MF [8] and, for half-integer ν, can be written as

$$\rho_{xx}\rho_{yy} = \left(\frac{h}{e^2} \right)^2 \frac{1}{(2\nu^2 + 1/2)^2}. \quad (11)$$

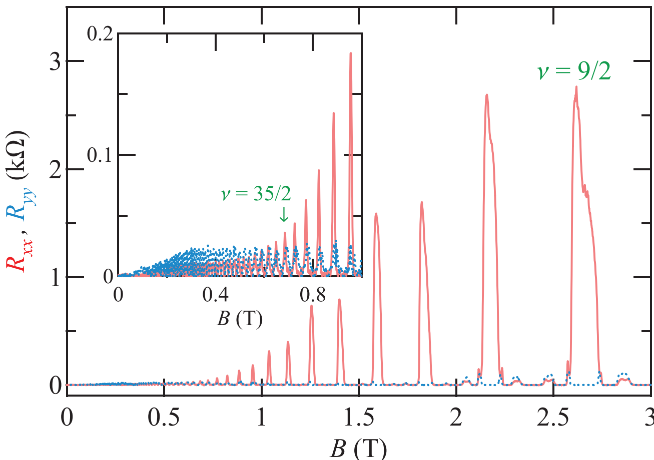

FIG. 3. R_{xx} (solid line) and R_{yy} (dotted line) as a function of B measured in sample A at $T \approx 50$ mK.

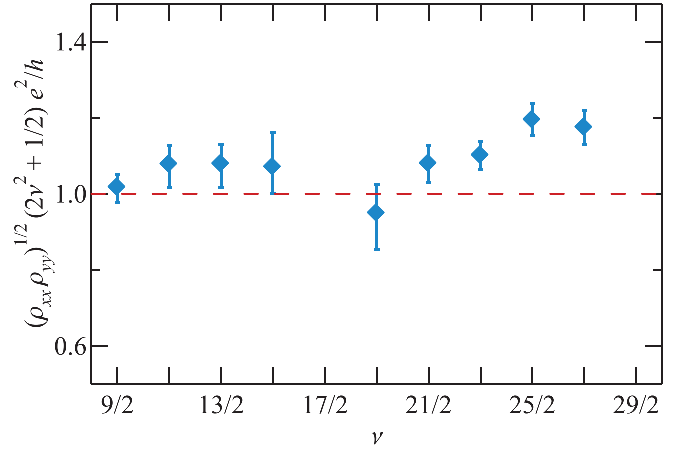

FIG. 4. $(\rho_{xx}\rho_{yy})^{1/2}(2\nu^2 + 1/2)e^2/h$ obtained using Eq. (9) from R_{xx} and R_{yy} measured in sample B (diamonds) and prescribed by Eq. (11) (dashed line) vs ν.

This result, together with Eq. (9), allows one to obtain the resistivity anisotropy ratio from R_{xx} alone,

$$R_{xx} = \frac{2h}{\pi e^2} \frac{\sum_{n=\mathrm{odd}^+} \left[n \sinh\left(\frac{\pi n}{2\sqrt{\rho_{xx}/\rho_{yy}}} \right) \right]^{-1}}{\nu^2 + 1/4}. \quad (12)$$

While the validity of Eq. (11) has been demonstrated long ago [12], it is instructive to check it again. In Fig. 4 we present $(\rho_{xx}\rho_{yy})^{1/2}(2\nu^2 + 1/2)e^2/h$, obtained from Eq. (9) using R_{xx} and R_{yy} measured in sample B, as a function of ν and observe that it stays close to unity as prescribed by Eq. (11) (dashed line). Given the fact that Eq. (11) has no adjustable parameters, the agreement is excellent and we will thus resort to using Eq. (12) when R_{yy} cannot be reliably obtained.

We next compare our main theoretical result, Eq. (4), to the experimental resistivity ratio ρ_{xx}/ρ_{yy} in sample A obtained using both methods. In Fig. 5 we present ρ_{xx}/ρ_{yy} obtained from experimental resistances using Eq. (10) (solid triangles) and Eq. (12) (open triangles) as a function of $[(2N+1)\nu]^{-2}$ over a wide range of half-integer ν, $9/2 \leqslant \nu \leqslant 35/2$. We observe that the values of ρ_{xx}/ρ_{yy} obtained by different methods in general agree with each other. The solid line is computed using Eq. (4) with $\gamma = 0.15$; it shows excellent agreement with the data for $13/2 \leqslant \nu \leqslant 35/2$. At $\nu \leqslant 11/2$, however, we find that Eq. (4) predicts ρ_{xx}/ρ_{yy} which is considerably higher than what is observed in our experiment. This trend is shared among all of our samples studied and we will return to this issue later.

Having looked at the dependence of ρ_{xx}/ρ_{yy} on ν and N, we next add its dependence on n_e and μ in the scaling (see Fig. 6). Here, we show the resistivity ratio ρ_{xx}/ρ_{yy} obtained from Eq. (10) (solid symbols) and Eq. (12) (open symbols) for samples A, B, and C (see legend) as a function of $[\hbar n_e\mu/\pi^3 e\nu(2N+1)]^2 = [\hbar\sigma_0/\pi^3 e^2\nu(2N+1)]^2$, where σ_0 is the conductivity at $B = 0$. At $N \geqslant 3$, the experimental points of Fig. 6 are close to a line computed using Eq. (4) with $\gamma = 0.15$. For $N = 2$, however, we see a substantial downward deviation of the data from this line. This is not surprising since we used Eq. (5) with β calculated for $N \gg 1$. Because $\rho_{xx}/\rho_{yy} \propto \beta^4$, only a 40% reduction of β by quantum

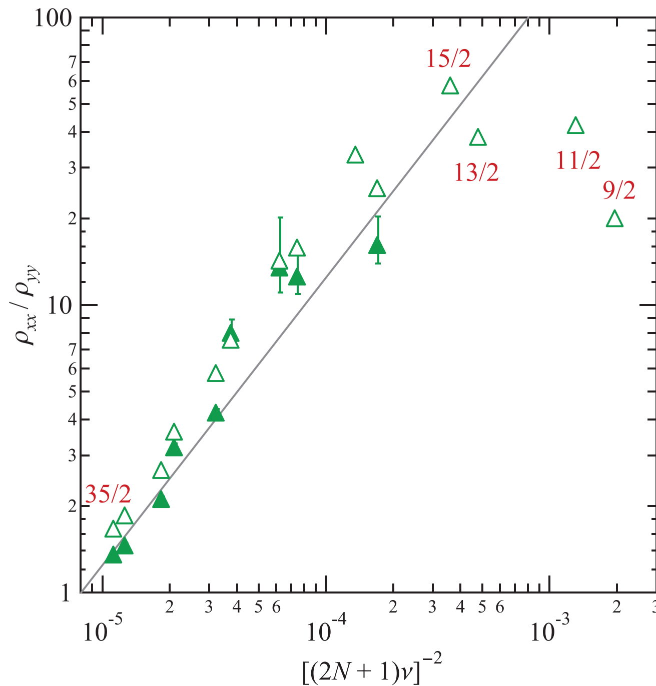

FIG. 5. Resistivity ratio ρ_{xx}/ρ_{yy} in sample A obtained from Eq. (10) (solid symbols) and Eq. (12) (open symbols) as a function of $[(2N+1)\nu]^{-2}$. Half integers mark filling factors. The line represents Eq. (4) with $\gamma = 0.15$.

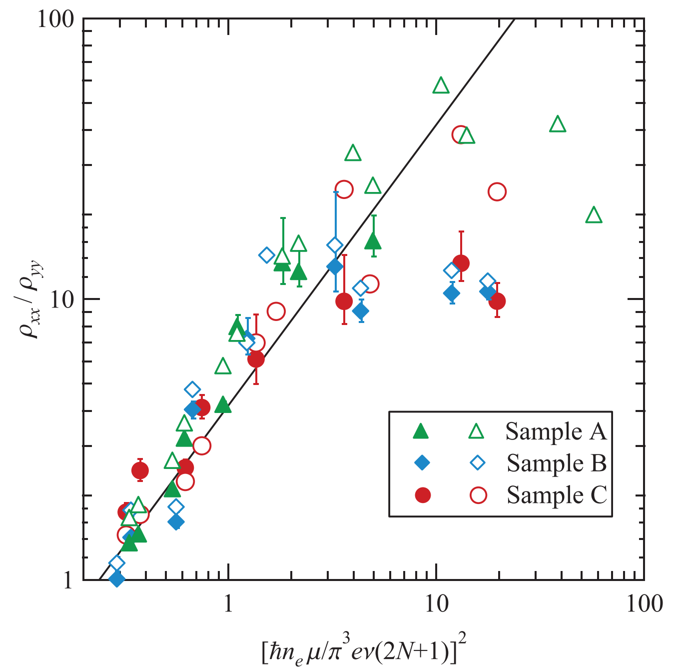

FIG. 6. Resistivity ratio ρ_{xx}/ρ_{yy} in sample A (triangles), B (diamonds), and C (circles) obtained from Eq. (10) (solid symbols) and Eq. (12) (open symbols) as a function of a scaling variable $[\hbar n_e \mu/\pi^3 e\nu(2N+1)]^2$. The line represents Eq. (4) with $\gamma = 0.15$.

fluctuations would explain the downward deviation of $N = 2$ points.

Using $\gamma = 0.15$ and Fig. 2 we find that $N_1/N_2 \simeq 60$. This is in reasonable agreement with $N_1/N_2 \sim 10$ obtained previously in Ref. [13] from the analysis of mobility and quantum mobility of an ultrahigh mobility sample of similar design. As mentioned in Ref. [13], the large value of N_1/N_2 is likely related to a relatively impure Al source [14]. With $N_1/N_2 \simeq 60$ and scattering rates $1/\tau$ and $2/\tau_B$ calculated for both types of impurities in the Supplemental Material [Eqs. (S1) and (S2)], we can estimate concentrations N_1 and N_2 and their relative contributions to both rates. We find that for sample A, the spacer impurities have concentration $N_1 \simeq 5 \times 10^{14}$ cm^{-3} and contribute 30%–40% to $2/\tau_B$ and 70%–80% to $1/\tau$, while GaAs well impurities have a concentration $N_2 \simeq 10^{13}$ cm^{-3} and contribute 60%–70% to $2/\tau_B$ and 20%–30% to $1/\tau$.

The agreement between our Eq. (4) and the experimental hard-to-easy resistivity ratios $\rho_{xx}/\rho_{yy} \lesssim 30$ for a large range of parameters supports the MF assumption that the low-temperature stripe phase is a pinned smectic phase predicted by HF calculations [1–3]. Apparently, at least for $N \geqslant 3$, there is no evidence for the role of pinned or free dislocations and other large defects conjectured in Refs. [15–17]. These conclusions agree with the recent observation of a possible nematic-smectic transition at $T \lesssim 50$ mK [18].

We thank I. Dmitriev and M. Fogler for discussions, and G. Jones, T. Murphy, and A. Bangura for technical support. Calculations by M.S. and Y.H. were supported primarily by the NSF through the University of Minnesota MRSEC under Award No. DMR-1420013. Experiments by X.F. and M.Z. were supported by the US Department of Energy, Office of Science, Basic Energy Sciences, under Award No. ER 46640-SC0002567. Growth of GaAs/AlGaAs quantum wells at Purdue University was supported by the US Department of Energy, Office of Science, Basic Energy Sciences, under Award No. DE-SC0006671. Growth of GaAs/AlGaAs quantum wells at Princeton University was supported by the Gordon and Betty Moore Foundation Grant No. GBMF 4420, and by the National Science Foundation MRSEC Grant No. DMR-1420541. A portion of this work was performed at the National High Magnetic Field Laboratory, which is supported by National Science Foundation Cooperative Agreements No. DMR-1157490 and No. DMR-1644779, and the State of Florida.

[1] A. A. Koulakov, M. M. Fogler, and B. I. Shklovskii, Phys. Rev. Lett. **76**, 499 (1996).
[2] M. M. Fogler, A. A. Koulakov, and B. I. Shklovskii, Phys. Rev. B **54**, 1853 (1996).
[3] R. Moessner and J. T. Chalker, Phys. Rev. B **54**, 5006 (1996).
[4] C. Wexler and A. T. Dorsey, Phys. Rev. B **64**, 115312 (2001).
[5] E. H. Rezayi, F. D. M. Haldane, and K. Yang, Phys. Rev. Lett. **83**, 1219 (1999).

[6] M. P. Lilly, K. B. Cooper, J. P. Eisenstein, L. N. Pfeiffer, and K. W. West, Phys. Rev. Lett. **82**, 394 (1999).
[7] R. R. Du, D. C. Tsui, H. L. Stormer, L. N. Pfeiffer, K. W. Baldwin, and K. W. West, Solid State Commun. **109**, 389 (1999).
[8] A. H. MacDonald and M. P. A. Fisher, Phys. Rev. B **61**, 5724 (2000).
[9] I. A. Dmitriev, A. D. Mirlin, and D. G. Polyakov, Phys. Rev. Lett. **91**, 226802 (2003).
[10] See Supplemental Material at http://link.aps.org/supplemental/10.1103/PhysRevB.100.241303 for calculation of $\gamma(N_1/N_2)$.
[11] S. H. Simon, Phys. Rev. Lett. **83**, 4223 (1999).
[12] J. P. Eisenstein, M. P. Lilly, K. B. Cooper, L. N. Pfeiffer, and K. W. West, Physica E **9**, 1 (2001).
[13] M. Sammon, M. A. Zudov, and B. I. Shklovskii, Phys. Rev. Materials **2**, 064604 (2018).
[14] Y. J. Chung, K. W. Baldwin, K. W. West, M. Shayegan, and L. N. Pfeiffer, Phys. Rev. Materials **2**, 034006 (2018).
[15] E. Fradkin and S. A. Kivelson, Phys. Rev. B **59**, 8065 (1999).
[16] E. Fradkin, S. A. Kivelson, E. Manousakis, and K. Nho, Phys. Rev. Lett. **84**, 1982 (2000).
[17] F. von Oppen, B. I. Halperin, and A. Stern, Phys. Rev. Lett. **84**, 2937 (2000).
[18] Q. Qian, J. Nakamura, S. Fallahi, G. C. Gardner, and M. J. Manfra, Nat. Commun. **8**, 1536 (2017).